Copyright © 2009 Year IEEE. Reprinted from the Journal of ELECTRONIC MATERIALS, Vol. 38, No. 1, 2009. This material is posted here with permission of the IEEE. Such permission of the IEEE does not in any way imply IEEE endorsement of any of Institute of Microelectronics' products or services. Internal or personal use of this material is permitted. However, permission to reprint/republish this material for advertising or promotional purposes or for creating new collective works for resale or redistribution must be obtained from the IEEE by writing to pubs-permission@ieee.org.

Journal of ELECTRONIC MATERIALS, Vol. 38, No. 1, 2009 *Special Issue Paper*
DOI: 10.1007/s11664-008-0565-6
© 2008 TMS

Effect of Electromigration on the Mechanical Performance of Sn-3.5Ag Solder Joints with Ni and Ni-P Metallizations

ADITYA KUMAR,[1,2] YING YANG,[1] CHEE C. WONG,[1] VAIDHYANATHAN KRIPESH,[2] and ZHONG CHEN[1,3]

1.—School of Materials Science and Engineering, Nanyang Technological University, 50 Nanyang Avenue, Singapore 639798, Singapore. 2.—Institute of Microelectronics, A*STAR (Agency for Science, Technology and Research), 11 Science Park Road, Singapore Science Park II, Singapore 117685, Singapore. 3.—e-mail: aszchen@ntu.edu.sg

The effect of moderate electric current density (1×10^3 to 3×10^3 A/cm^2) on the mechanical properties of Ni-P/Sn-3.5Ag/Ni-P and Ni/Sn-3.5Ag/Ni solder joints was investigated using a microtensile test. Thermal aging was carried out at 160°C for 100 h while the current was passed. The interfacial microstructure and intermetallic compound (IMC) growth were analyzed. It was found that, at these levels of current density, there were no observable voids or hillocks. Samples aged at 160°C without current stressing failed mostly inside the bulk solder with significant prior plastic deformation. The passage of current was found to cause brittle failure of the solder joints and this tendency for brittle failure increased with increasing current density. Fractographic analysis showed that, in most of the electrically stressed samples, fracture occurred at the interface region between the solder and the joining metals. The critical current density that caused brittle fracture was about 2×10^3 A/cm^2. Once brittle fracture occurred, the tensile toughness, defined as the energy per unit fractured area, was usually lower than ~5 kJ/m^2, compared with the case of ductile fracture where this value was typically greater than ~9 kJ/m^2. When comparing the two types of joint, the brittle failure was found to be more severe with the Ni than with the Ni-P joint. This work also found that the passage of electric current affects the IMC growth rate more significantly in the Ni than in the Ni-P joint. In the case of the Ni joint, the Ni_3Sn_4 IMC at the anode side was appreciably thicker than that formed at the cathode side. However, in the case of electroless Ni-P metallization, this difference was much smaller.

Key words: Electromigration, lead-free solder, interfacial reactions, metallization, intermetallic compound (IMC), tensile strength

INTRODUCTION

The trend towards increasing input/output (I/O) density requires finer pitch and smaller solder ball size in flip-chip and ball grid array (BGA) packages. As a result, the density of electric current passing through the solder interconnects is increasing. High current density poses the potential risk of electrical failure in solder joints due to electromigration. In an actual flip-chip joint, for example, current crowding may further increase the current density at the corner of the solder near the pad metallization.[1,2] So far, the majority of the research work on electromigration-induced package failure intentionally used current densities on the order of 10^4 A/cm^2 in order to observe package failure after a short period. At this level of current density, voids and hillocks can be observed at the cathode and anode sides, respectively. However, this accelerated test may not

(Received March 17, 2008; accepted September 8, 2008; published online November 1, 2008)

be the best representation of what happens in an actual package, in which the current density may be lower. So far limited research has found that, even at moderate current density (~10^3 A/cm^2), electromigration can still affect intermetallic compound (IMC) formation.[3,4] In a review article, Conrad[5] presented several examples in which electric current at the level of 10^3 A/cm^2 influences IMC formation, particle precipitation, recrystallization, and grain coarsening in different material systems.[5] As the microstructural changes affect the mechanical properties of the solder joint, it is of great interest to study the effect of electric current on the mechanical properties of solder joints at moderate current densities. A recent article by Ren et al.[6] showed that, in a 95.5Sn-3.8Ag-0.7Cu solder joint with copper wires, aging at 145°C coupled with the passage of a direct current at a density of 5×10^3 A/cm^2 caused brittle failure at the cathode interface.

Ni-based metallizations, such as electrolessly plated Ni-P alloy and high-purity electroplated Ni, have been proven to have slower reactions with high-Sn-containing lead-free solders than do copper or copper-based metallizations. There have been quite a number of studies on the morphology of the interface IMC between Ni-based metallizations and Sn-bearing solders and the corresponding growth kinetics.[7–17] Among the Ni-based metallizations, electrolessly plated Ni-P is an amorphous alloy of Ni, containing 6 wt.% to 13 wt.% P. This alloy has attracted a great deal of attention in the electronic packaging industry because of its low facility setup cost, good selectivity, and the conformity of the coatings. On the other hand, electroplated pure Ni has also been widely used as a substrate metallization because of its fast plating rate and the stability of plating quality. In this study, the effect of electric current on the interfacial microstructure and tensile joint strength of electroless Ni-P and Ni with lead-free Sn-3.5Ag solder was investigated with particular interest on the effect of moderate current stressing (~10^3 A/cm^2). The samples prepared were aged at 160°C for 100 h at a current density of 1×10^3 A/cm^2, 2×10^3 A/cm^2, or 3×10^3 A/cm^2. After thermal aging, tensile testing was performed. Interfacial microstructure and fractographic analyses were carried out using a scanning electron microscope. Emphasis was placed on the relation between current density and mechanical degradation of the solder joint. It is noted that studies on joint strength have mainly been carried out by shear testing in the past[18,19] due to the ease of this testing approach. Our group started using microtensile testing[20–23] to assess joint strength degradation. Tensile testing can better preserve the fractured surface for subsequent fractographic analysis. In addition, since the stress distribution in all interface layers is the same, tensile testing can be used to reveal the weakest layer or interface better than shear testing. Therefore from the point of view of studying the failure mechanism, microtensile testing has an advantage over shear testing.

EXPERIMENTAL PROCEDURE

Microtensile test samples with either Ni-P or Ni metallizations, joined by lead-free Sn-3.5Ag solder, were prepared following the procedure described in our previous work.[23] The electroless Ni-P/Sn-3.5Ag test samples were prepared by first plating electroless Ni-P (16 at.% P, 9.9 μm thick) and immersion Au (~50 nm) on a surface-cleaned Cu plate (purity 99.98 wt.%). Two pieces of 6-mm-thick plates were joined using Sn-3.5Ag solder wires at 250°C for 60 s. The joined plates were cut through their thickness into many small pieces of Ni-P/Sn-3.5Ag/Ni-P samples using a diamond saw cutter. First, the joined plate was cut into thin slices along one of the directions in the plane of the plate (say, the x-axis of the x–y plane). Then the thin slices were cut again along the y-axis to produce many microtensile test samples. In order to ensure minimum damage to the sample during cutting, the thin slices produced during the first cutting were glued together by a room-temperature-cure adhesive before the second cutting. The adhesive can be easily removed by soaking in acetone afterwards. The dimensions of the final test samples are shown in Fig. 1a. For the Ni/Sn-3.5Ag/Ni samples, a similar preparation method was followed using Ni plates (purity 99.98 wt.%) instead of Cu plates. Immersion Au was also plated on the etched and cleaned Ni plate surface before the joining. Figure 1b shows a schematic diagram of the Ni/Sn-3.5Ag/Ni test samples.

The as-prepared samples were heated in an oven at 160°C for 100 h with a direct electric current applied at a density of 1×10^3 A/cm^2, 2×10^3 A/cm^2, or 3×10^3 A/cm^2. For comparison, samples aged at 160°C for 100 h without passing a current were also prepared. After the aging treatment, samples were removed from the oven and cooled in air to room temperature.

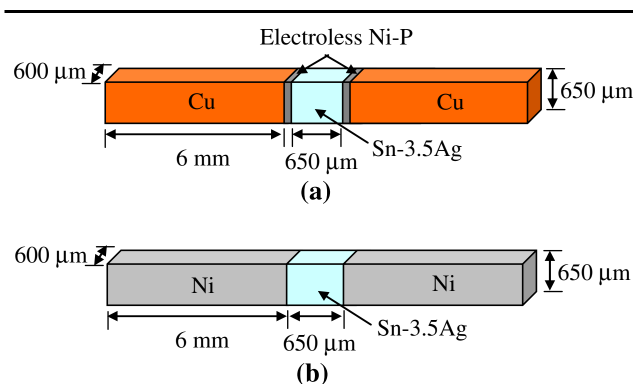

Fig. 1. Schematic diagram of (a) Ni-P/Sn-3.5Ag/Ni-P and (b) Ni/Sn-3.5Ag/Ni microtensile samples.

The applied electric current results in Joule heating, hence the increase in temperature due to electrical stressing was measured with the help of a thermocouple adhered to the joint interface region. For all our experiments, the increase in temperature was small. A maximum increase of around 5°C was observed at the highest (3×10^3 A/cm^2) current density. This small increase in temperature due to the passage of electric current was negligible compared with the thermal aging temperature of 160°C.

Tensile testing was performed using an INSTRON 5567 mechanical tester. Five samples for each condition were tested at room temperature with a constant crosshead speed of 0.05 mm/min. The load–displacement curve was recorded for each test. The tensile strength was given by the maximum load divided by the measured cross-sectional area of the solder joint. The fracture energy was obtained by the area under the load–displacement curve up to the point of specimen separation. Tensile toughness was defined as the fracture energy per unit cross-sectional area of test sample. This term is used to differentiate it from another term, fracture toughness, which has been well defined in fracture mechanics.

A JEOL JSM-6360A scanning electron microscope (SEM) was used for microstructure and fractographic analyses. For the cross-sectional SEM, the samples were cold-mounted in epoxy and polished down to a 1-μm finish. After polishing, solder etching was carried out with 4 vol.% HCl acid for a few seconds to reveal the microstructure. Energy-dispersive x-ray (EDX) spectroscopy was performed in the SEM to analyze chemical composition. Image processing and analysis software was used to measure the area and length of the IMC layer from the SEM images. The average thickness of the IMC layer was determined by dividing the area by the length. In the samples aged by passing a current, the thickness was measured at both the anode-side interface (where electrons flow from solder to metallization) and the cathode-side interface (where electrons flow from metallization to solder). In the samples aged without current passing, the IMC thickness at both the interfaces were nearly the same; therefore the average value of both sides was reported.

RESULTS AND ANALYSIS

Tensile Testing

Figure 2 shows the tensile strength of Ni-P/Sn-3.5Ag/Ni-P and Ni/Sn-3.5Ag/Ni joints as a function of current density. Thermal aging without the passage of current is counted as zero current density. Both individual strengths and the average value are provided in the same plot. Both types of joints showed a large variation at a current density of 2×10^3 A/cm^2 and 3×10^3 A/cm^2. When the variation was large, the average strength of only five specimens may not be very meaningful. Thus detailed analysis of the fracture mode and the fracture energy of individual test samples is needed. With thermal aging only and with a low current density of 1×10^3 A/cm^2, the five data points were relatively close, making the average value meaningful. The average tensile strength of both types of joints was ~50 MPa without current stressing. It increased slightly for the Ni-P solder joint but declined slightly for the Ni solder joint from no current to 1×10^3 A/cm^2.

The fracture energy of the solder joints is plotted as a function of current density in Fig. 3. For the Ni-P joint, the samples aged without current stressing and those with 1×10^3 A/cm^2 current density showed consistent fracture energy in the group. A large amount of data scatter occurred at the 2×10^3 A/cm^2 and 3×10^3 A/cm^2 current densities. For the Ni joint, a large variation appeared in the no-current and low-current-density (1×10^3 A/cm^2) groups (Fig. 3b). For the high-current-density groups (2×10^3 A/cm^2 and 3×10^3 A/cm^2), the fracture energy was consistently low, thus with a small variation within the groups. The general trend is for the average fracture energy of both types of solder joints to decrease with increasing current density. Although the strength data (Fig. 2b) showed a small variation of the Ni solder joint for the sample that was aged only thermally

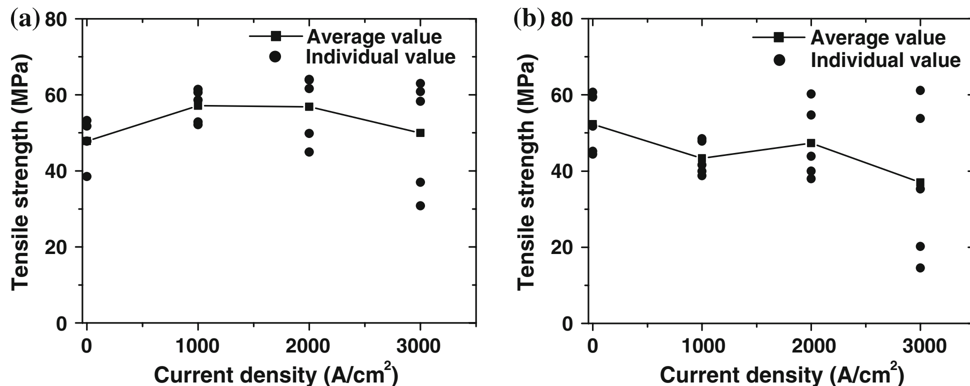

Fig. 2. Tensile strength of (a) Ni-P/Sn-3.5Ag/Ni-P and (b) Ni/Sn-3.5Ag/Ni solder joints as a function of current density.

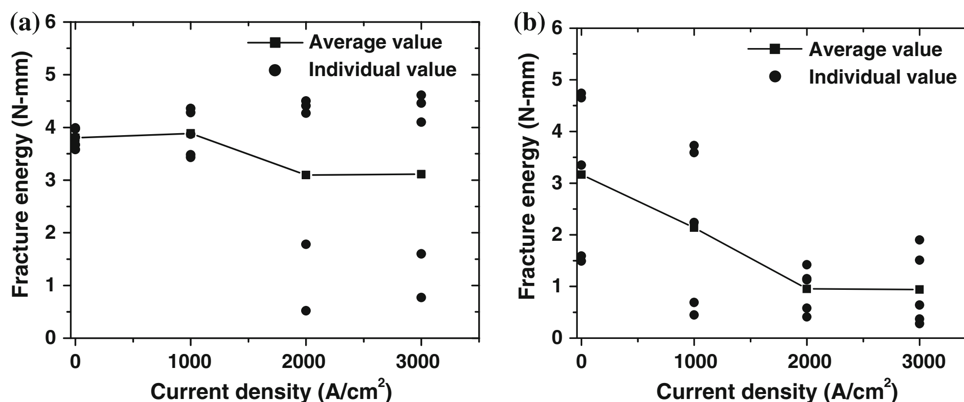

Fig. 3. Fracture energy of (a) Ni-P/Sn-3.5Ag/Ni-P and (b) Ni/Sn-3.5Ag/Ni solder joints as a function of current density.

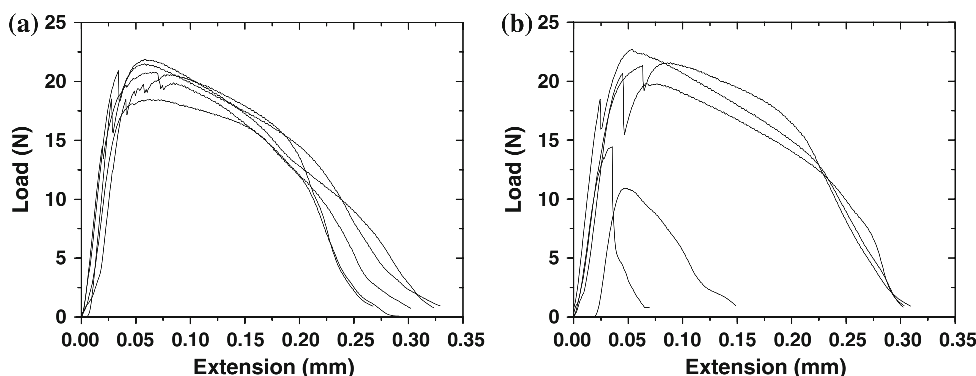

Fig. 4. Load–displacement curves of the Ni-P/Sn-3.5Ag/Ni-P solder joints aged with (a) 1×10^3 A/cm^2 and (b) 3×10^3 A/cm^2 current densities.

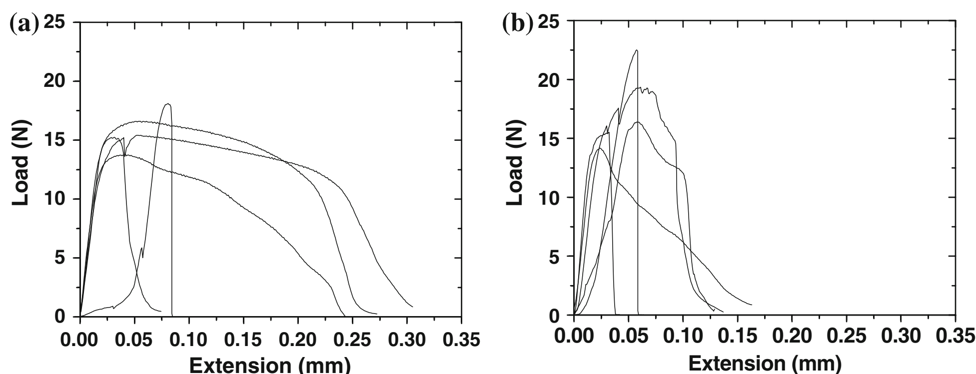

Fig. 5. Load–displacement curves of the Ni/Sn-3.5Ag/Ni solder joints aged with (a) 1×10^3 A/cm^2 and (b) 2×10^3 A/cm^2 current densities.

and the low-current-density group, the fracture energy showed the opposite effect. Therefore to understand the mechanical behavior fully, the full load–displacement history has to be analyzed.

Figure 4 displays the load–displacement curves of the five Ni-P samples tested at 1×10^3 A/cm^2 and 3×10^3 A/cm^2. The curves for the aged-only samples exhibit similar patterns to those shown in Fig. 4a, and thus Fig. 4a also represents the test record of the no-current samples. Basically in both the no-current and low-current-density groups, all tested samples exhibited significant amounts of plastic deformation in the solder prior to fracture. This is verified later in the fractured sample images. In Fig. 4b, however, it is clear that, out of five tested samples, only three remained ductile. The other two broke at a much lower strength and ductility, leading to brittle behavior with lower fracture energies. The representative curves for the Ni solder joints shown in Fig. 5, however, exhibit different patterns. In the no-current and low-current-density groups (1×10^3 A/cm^2), two samples in each group displayed brittle behavior (Figs. 5a and 3b) even though their breaking load

remained high (Figs. 5a and 2b). In the high-current-density groups, all five samples exhibited little deformation prior to failure (Fig. 5b).

Overall, it was observed that, for ductile fracture of both types of solder joints, the fracture energy is above 3.5 N mm, which gives rise to a tensile toughness equal to or greater than ~9 kJ/m^2. On the other hand, in brittle fracture the energy is consistently lower than 2.0 N mm, translating into a tensile toughness of less than ~5 kJ/m^2.

Fracture Path Analysis

In all the Ni-P/Sn-3.5Ag/Ni-P samples aged without current or with low current density (1 × 10^3 A/cm^2), failure was ductile and the fracture path was inside the bulk solder (Fig. 6). However in the case of higher current densities (2 × 10^3 A/cm^2 and 3 × 10^3 A/cm^2), two out of the five samples exhibited brittle failure. In the case of brittle failure, the fracture was primarily at the Ni_3Sn_4/Sn-3.5Ag interface (Fig. 7). The broken interface was observed at both the cathode side and the anode side, therefore it appears there is no clear polarity effect at this current density level. This point needs further clarification using a larger number of samples for each condition, which was not done in the current study. Figure 8 shows a top view of the broken surfaces of the same sample shown in Fig. 7. The separation between equiaxial Ni_3Sn_4 particles and the solder matrix is clearly observable, leaving large shallow dimples at the interface.

In the case of the Ni/Sn-3.5Ag/Ni samples, three of the five samples that were aged without passing current exhibited ductile fracture inside the bulk solder (Fig. 9), whereas the other two exhibited brittle fracture at the solder/IMC interface region (Fig. 10). The fracture path was found to be a combination of solder/IMC interface, inside the IMC layer, and IMC/Ni interface. A similar pattern was found in the samples from the low-current-density (1 × 10^3 A/cm^2) group. The tendency for brittle fracture increased with increasing current density. All five samples that were aged with the current densities of 2 × 10^3 A/cm^2 and 3 × 10^3 A/cm^2 exhibited brittle fracture with low fracture energy (Fig. 11). Similar to the Ni-P/Sn-3.5Ag/Ni-P samples, fracture at both the cathode and anode ends was observed. Due to the small number of samples tested, no conclusion on polarity effect could be made for the brittle failure of Ni/Sn-3.5Ag/Ni joints.

Microstructure Analysis

Figure 12 shows cross-sectional SEM images of electroless Ni-P/Sn-3.5Ag interfaces for the sample aged at 160°C for 100 h without current stressing. Both Ni_3Sn_4 and Ni_3P compounds formed during the aging process. The interface between the Ni_3Sn_4 IMC and the Sn-3.5Ag solder was very uneven, typical of Ni-P/Sn-3.5Ag reaction. In the electrically stressed sample (Fig. 13), the same compounds

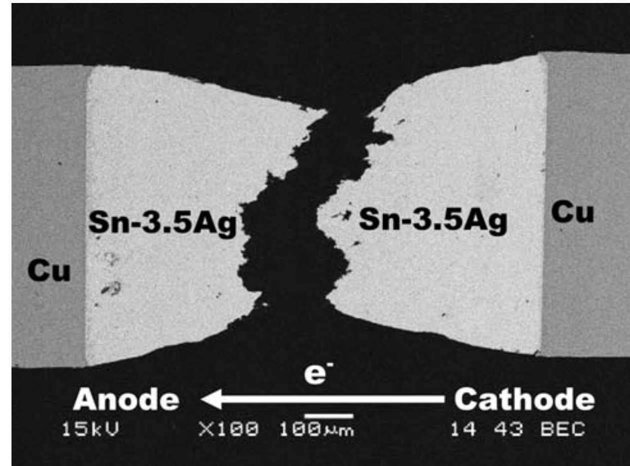

Fig. 6. SEM image showing fracture in the Ni-P/Sn-3.5Ag/Ni-P sample aged at 160°C for 100 h with a current of 1 × 10^3 A/cm^2 density. Neck formation in the bulk solder indicates ductile failure of the solder joint.

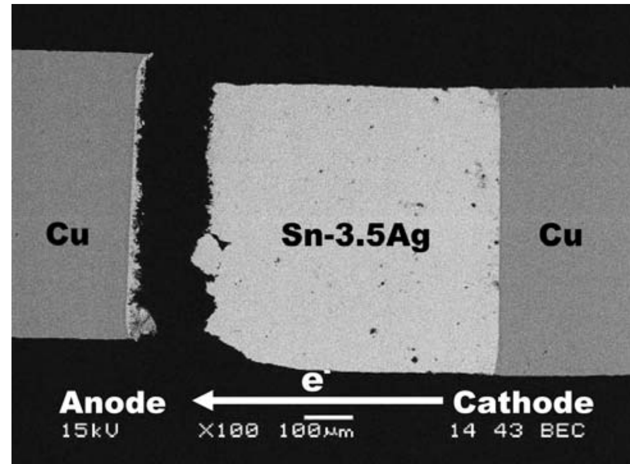

Fig. 7. SEM image showing brittle fracture in the Ni-P/Sn-3.5Ag/Ni-P sample aged at 160°C for 100 h with current density 3 × 10^3 A/cm^2. The brittle failure occurred at the Ni_3Sn_4/Sn-3.5Ag interface.

(Ni_3Sn_4 and Ni_3P) were observed and the Ni_3Sn_4/Sn-3.5Ag interface was very rough, too. No significant difference was observed in the thickness and shape of Ni_3Sn_4 IMCs at the anode and cathode side.

In the case of the Ni/Sn-3.5Ag/Ni joint, only one IMC, Ni_3Sn_4, was present at the interface. Compared with the electroless Ni-P/Sn-3.5Ag samples, the Ni_3Sn_4/Sn-3.5Ag interface was relatively smooth. Another difference observed was the greater thickness of Ni_3Sn_4 IMC grown at the anode side Ni/Sn-3.5Ag interface than that of Ni_3Sn_4 IMC at the cathode side. This is clearly observable by comparing the interface without current (Fig. 14) and the one with current passing (Fig. 15).

The measured thickness of Ni_3Sn_4 IMC in the samples aged at 160°C for 100 h, as a function of

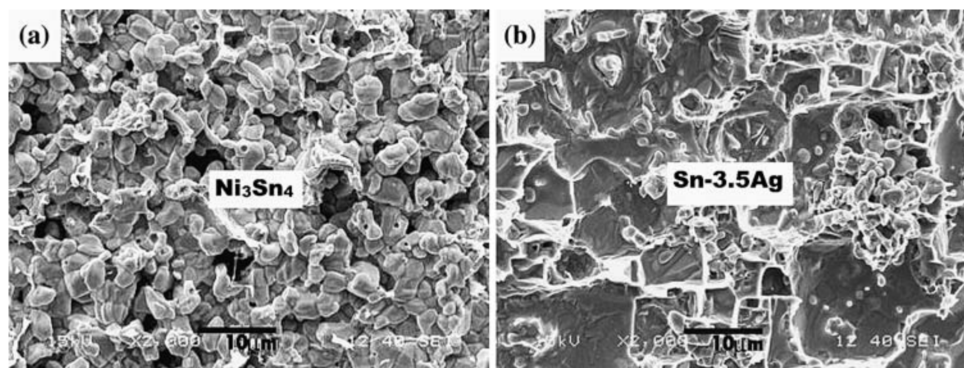

Fig. 8. Top view of the fracture surfaces of the sample shown in Fig. 7: (a) left-hand side surface and (b) right-hand side surface.

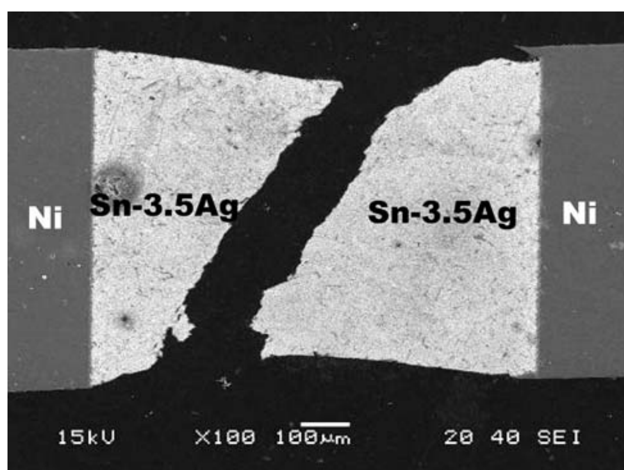

Fig. 9. Fracture in the Ni/Sn-3.5Ag/Ni sample aged at 160°C for 100 h without current, showing ductile failure inside the bulk solder.

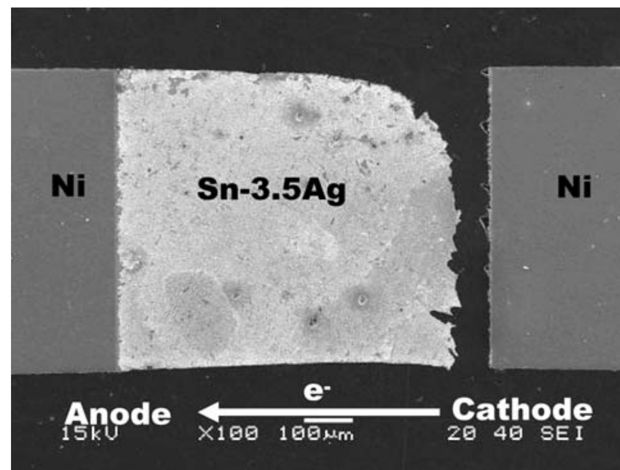

Fig. 11. SEM images showing fracture in the Ni/Sn-3.5Ag/Ni joint after aging at 160°C for 100 h with passage of a current density of 2×10^3 A/cm^2.

current density is shown in Fig. 16. Electric current influenced the Ni_3Sn_4 IMC growth significantly in the Ni/Sn-3.5Ag/Ni sample (Fig. 16b), whereas its effect was small or nearly negligible in the Ni-P/Sn-3.5Ag/Ni-P sample (Fig. 16a). In the Ni samples, the thickness of Ni_3Sn_4 IMC that formed at the anode side Ni/Sn-3.5Ag interface increased with increasing current density, whereas the thickness of Ni_3Sn_4 IMC that formed at the cathode side Ni/Sn-3.5Ag interface decreased slightly with current density. On the other hand, in the electroless Ni-P/Sn-3.5Ag samples, no significant difference was

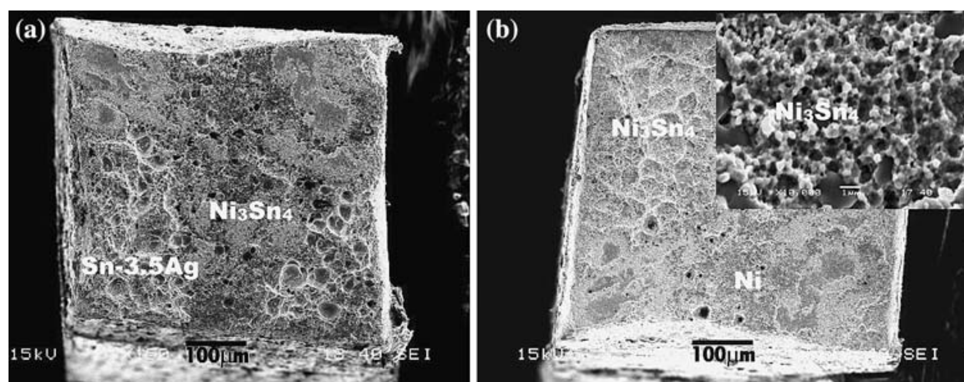

Fig. 10. Fracture surfaces of the broken Ni/Sn-3.5Ag/Ni joint after aging at 160°C for 100 h without current. Observed from (a) the solder side and (b) the Ni side. The brittle fracture takes a combined path of Sn-3.5Ag/Ni_3Sn_4, within Ni_3Sn_4 layer, and Ni_3Sn_4/Ni. The inset shows a magnified view of Ni_3Sn_4 IMCs.

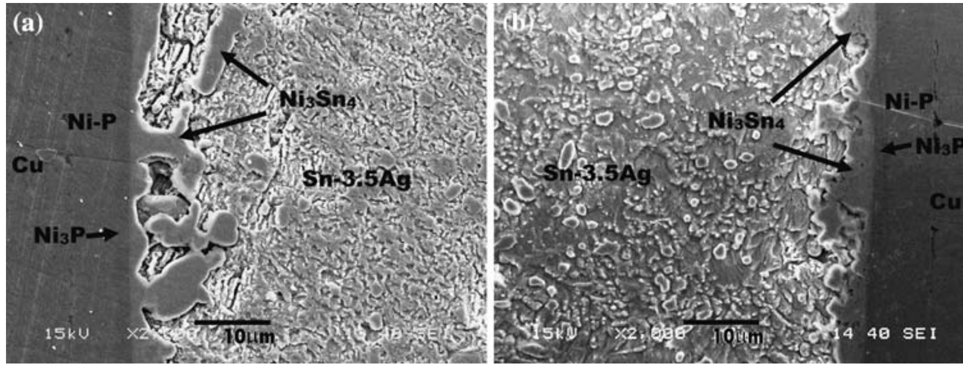

Fig. 12. Cross-sectional SEM images of Ni-P/Sn-3.5Ag/Ni-P interfaces of the sample aged at 160°C for 100 h without current. An example of (a) the left-hand side and (b) the right-hand side of the same joint.

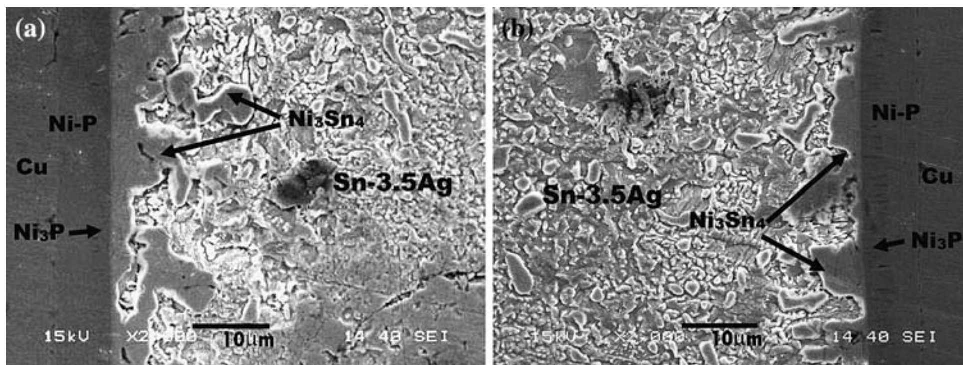

Fig. 13. Cross-sectional SEM images of Ni-P/Sn-3.5Ag/Ni-P interfaces of the sample aged at 160°C for 100 h with passage of current density of 2×10^3 A/cm^2: (a) anode side and (b) cathode side.

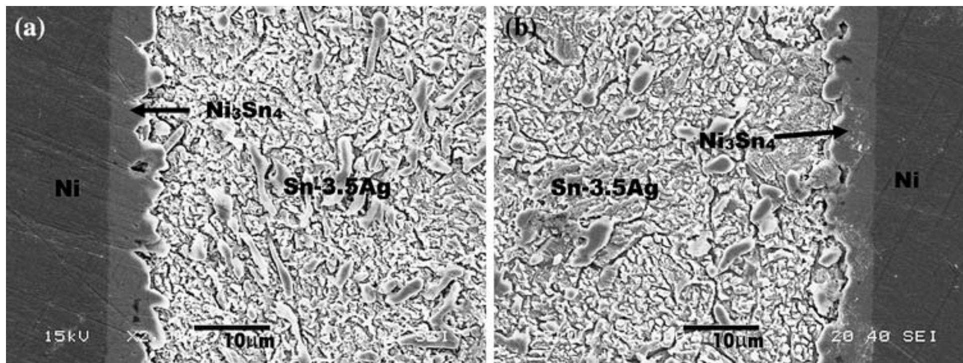

Fig. 14. Cross-sectional SEM images of Ni/Sn-3.5Ag/Ni interfaces of the sample aged at 160°C for 100 h without current. An example of (a) left-hand side and (b) right-hand side interface.

observed in the thickness of Ni_3Sn_4 IMC grown at both anode and cathode sides.

DISCUSSION

Effect of Electromigration on the Mechanical Properties of Solder Joints

In the current study, although no void and hillock formation was observed, the passage of electric current during aging treatment clearly had an impact on the mechanical performance of the solder joint. It was found that an electric current density of 2×10^3 A/cm^2 was sufficient to embrittle the solder joints. In both types of joints, the fracture mode exhibited a general trend for transition from ductile bulk solder failure to brittle interface failure with increasing current density. Based on the current work, the brittle interface failure could be due to two possible causes. One is that the interface has been weakened considerably due to extended

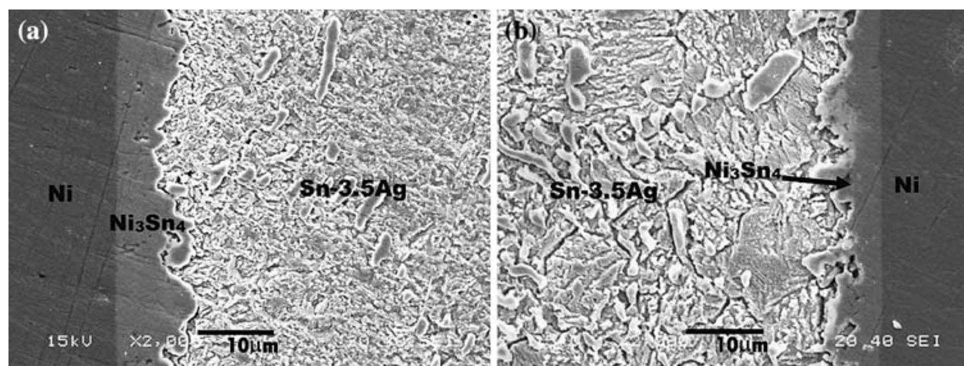

Fig. 15. Cross-sectional SEM images of Ni/Sn-3.5Ag/Ni interfaces of the sample aged at 160°C for 100 h with current density of 2×10^3 A/cm^2: (a) anode side and (b) cathode side.

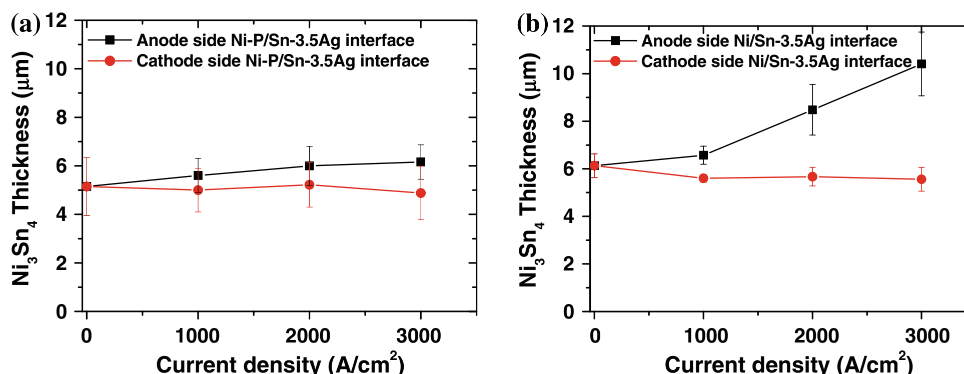

Fig. 16. Thickness of Ni_3Sn_4 IMC in the (a) Ni-P/Sn-3.5Ag and (b) Ni/Sn-3.5Ag joints aged at 160°C for 100 h, as a function of current density.

interface reaction, which leads to the decrease in both strength and fracture energy (e.g., Figs. 4b and 7). Indeed there is plenty of evidence for interface strength degradation with either extended aging or reflow.[20–26] The interface reaction was found to smoothen the interface and/or generate interface voids, causing the degradation. The passage of electric current is likely to aid interdiffusion during the interface reaction, expediting the degradation process. This kind of degradation could happen well before electromigration-induced voiding and can be very well revealed by the microtensile test used in our work.

The other cause could be the relative increase in bulk solder strength while the interface strength remains high. In other words, the interface is comparatively weakened. Comparing Fig. 5a and b, it is clear that some of the brittle fracture occurred at higher breaking loads than the bulk solder failure, but the energy under the load–displacement curves was much lower. Indeed it has been reported before that bulk solder strength can increase with thermal aging time when the aging temperature is no more than 160°C[25] or with reflow duration within a relatively short duration.[27] There has been no sound explanation for this increase so far, but we believe that it could be explained by increased dissolution of metallization metals into the bulk solder. Upon cooling, a greater volume fraction of IMC particles will precipitate out in the solder matrix, leading to an increase in solder strength. The passage of current assists the dissolution of metal pad into the solder matrix, thus increasing the bulk solder strength. In such a case, brittle fracture could happen at relatively high strength but low fracture energy.

The Ni solder joint was found to be less reliable compared with the electroless Ni-P solder joint; for example, among the thermally aged samples, although both types of joints had similar strength, some Ni/solder joints showed brittle interface failure with lower toughness, while no Ni-P joint exhibited such brittle failure. With current stressing at relatively high densities, all the Ni joints showed brittle failure, but some Ni-P joints remained ductile. This indicates that the interface in the Ni-P/Sn-3.5Ag solder joint possesses a greater resistance to thermal and electromigration degradation. Microstructure analyses of the interface revealed the presence of a relatively smooth Ni_3Sn_4/solder interface (Figs. 14 and 15) at the Ni/Sn-3.5Ag joint interface. Since a smooth Ni_3Sn_4/solder interface implies low mechanical interlocking, low initial interfacial toughness and faster degradation of the Ni/Sn-3.5Ag solder joint can be explained. On the other hand, the rough Ni_3Sn_4/Sn-3.5Ag interface formed in the case of electroless Ni-P metallization delays the electric-current-induced brittle failure of the electroless Ni-P/Sn-3.5Ag solder joint.

At this moderate current density ($\sim10^3$ A/cm^2), solder joint degradation has been clearly observed, but what happens at the microscopic level of the solder joint that has led to the degradation is still not clear. It is very tempting to suggest that, despite the fact that no voids or hillocks are formed at this level of current stressing, micropores, which are not observable by SEM, may still exist. If this is true, then the weakening should happen at the cathode end of the joint where these tiny voids would form. This will lead to the so-called polarity effect which has been exemplified by many researchers[28,29] using current density on the order of 10^4 A/cm^2. The lowest current density reported so far to cause brittle fracture with a clear polarity effect was 5×10^3 A/cm^2, which was found by Ren et al. in the Cu/95.5Sn-3.8Ag-0.7Cu solder joint.[6] In our work, although embrittlement caused by current stressing was confirmed, no polarity effect was observed at current densities up to 3×10^3 A/cm^2. Therefore, there might be other mechanisms of degradation in addition to the formation of micropores that causes the brittle fracture. We expect that, if the current density is further increased, a polarity effect might be present in our Ni-P and Ni joints as well, as in the case of Ren et al.[6] Understandably, since the Cu/Sn reaction is much faster than that of Ni/Sn, the critical current density to observe the polarity effect for the Ni-based joint might be higher than 5×10^3 A/cm^2. The importance of this work is to have revealed that, even before the polarity effect is dominant, electric current may have already caused solder joint degradation. The degradation mechanisms under this moderate current stressing range could be a complicated combination of several factors and requires further investigation.

Effect of Electric Current on Ni_3Sn_4 IMC Growth

In several studies,[3,4,30] electromigration has been reported to have affected the interfacial reactions in various metallic systems in terms of phase formation and IMC growth. In the current work, electromigration was also found to affect the growth of Ni_3Sn_4 IMCs in the Ni/Sn-3.5Ag sample (Fig. 16b); however, such an electromigration effect was relatively small or negligible in the Ni-P/Sn-3.5Ag sample (Fig. 16a). Moreover, the current passage did not change the type of IMC formed: the same IMC(s) formed during aging with or without electric current.

The growth of IMCs in a UBM/solder joint depends upon the direction of the atomic fluxes at the reaction interface. If atomic fluxes flowing toward the reaction interface are larger than the fluxes flowing outward, then the IMC grows; otherwise, it shrinks. Electromigration influences the atomic flux of species in heterogeneous materials systems; in most systems, electromigration increases the atomic flux of species when electrons flow in the direction of species diffusion driven by a concentration gradient, whereas it reduces the atomic flux of species when electrons flow in the opposite direction. In this study, it was observed that, in the Ni/Sn-3.5Ag solder joint, electromigration increases the Ni_3Sn_4 growth at the anode-side interface with increasing current density, whereas it suppresses the Ni_3Sn_4 growth at the cathode-side interface (Fig. 16b). A similar electromigration effect on the growth of Ni_3Sn_4 IMCs in the Ni/Sn-3.5Ag solder joint during aging at different temperatures was observed by Chen and Chen.[3] They found that electromigration influences the Sn flux through Ni_3Sn_4, whereas it does not have a significant affect on the Ni flux through Ni_3Sn_4. Thus in the Ni/Sn-3.5Ag solder joint, electromigration enhances the Ni_3Sn_4 growth at the anode-side interface by increasing the influx of Sn, whereas it suppresses the Ni_3Sn_4 growth at the cathode-side interface by reducing the influx of Sn.

On the other hand, in the electroless Ni-P/Sn-3.5Ag system, as reported in our previous work,[31] Ni_3Sn_4 grows at the interface between itself and a ternary Ni-Sn-P compound. Ni comes from the electroless Ni-P layer through the Ni_3P and Ni-Sn-P layers and Sn comes from the solder through the Ni_3Sn_4 layer. The presence of Ni_3P and Ni-Sn-P layers between electroless Ni-P and Ni_3Sn_4 layers plays an important role in defining the effect of electromigration on Ni_3Sn_4 growth. During the passage of electron current through the Ni-P/Sn-3.5Ag/Ni-P joint, at the anode-side interface, electromigration enhances the Sn flux through Ni_3Sn_4 but retards the Ni flux through Ni_3P, whereas at the cathode-side interface it retards the Sn flux but enhances the Ni flux. As a result, the net effect of electromigration on Ni_3Sn_4 growth in the Ni-P/Sn-3.5Ag/Ni-P solder joint is very limited.

CONCLUSIONS

In this study, the effect of moderate electric current density ($\sim10^3$ A/cm^2) on the mechanical properties and interfacial microstructure of Ni-P/Sn-3.5Ag/Ni-P and Ni/Sn-3.5Ag/Ni solder joints was investigated. The following conclusions can be drawn from this study:

1. Electric current induces brittle failure in both types of solder joints. The tendency for brittle failure increases with increasing current density. Under our test conditions, it was found that a current density at 2×10^3 A/cm^2 is sufficient to embrittle the solder joints. Below this density, there is no significant embrittlement effect.
2. The brittle fracture at the interface may be caused by either absolute degradation of the interface, or relative increase in the bulk solder strength, making the interface relatively weak. In this work, the interface in the Ni/Sn-3.5Ag/Ni solder joint was found to be relatively weak as compared with the Ni-P/Sn-3.5Ag/Ni-P solder

joint. In the Ni/Sn-3.5Ag/Ni joint, the brittle fracture followed a mixed crack propagation path through different interfaces, while in the case of the Ni-P/Sn-3.5Ag/Ni-P joint, the brittle fractures occurred mainly at the Ni_3Sn_4 IMC/solder interface. The fracture energy decreased more rapidly with the Ni joint as compared with the Ni-P joint. Overall, it has been observed that, for ductile fracture of both types of solder joints, the tensile toughness is greater than ~9 kJ/m^2 while that for brittle fracture is less than ~5 kJ/m^2.

3. The effect of electromigration on IMC growth depends on the type of metallization. In the case of Ni metallization, Ni_3Sn_4 IMC grows faster at the anode side than at the cathode side. In the case of electroless Ni-P metallization, electric current does not have a significant effect on Ni_3Sn_4 growth.

ACKNOWLEDGEMENTS

This work was supported by research Grants RG19/00 from Nanyang Technological University, Singapore, IME/04-220004 from Institute of Microelectronics/A*Star, Singapore, and JT ARC 2/03 from MOE/A*Star, Singapore.

REFERENCES

1. T.Y. Lee, K.N. Tu, and D.R. Frear, *J. Appl. Phys.* 90, 4502 (2001). doi:10.1063/1.1400096.
2. E.C.C. Yeh, W.J. Choi, K.N. Tu, P. Elenius, and H. Balkan, *Appl. Phys. Lett.* 80, 580 (2002). doi:10.1063/1.1432443.
3. C.M. Chen and S.W. Chen, *J. Appl. Phys.* 90, 1208 (2001). doi:10.1063/1.1380219.
4. H. Gan and K.N. Tu, *J. Appl. Phys.* 97, 063514 (2005). doi:10.1063/1.1861151.
5. H. Conrad, *Mater. Sci. Eng. A* 287, 227 (2000). doi:10.1016/S0921-5093(00)00780-2.
6. F. Ren, J.-W. Nah, K.N. Tu, B. Xiong, L. Xu, and J.H.L. Pang, *Appl. Phys. Lett.* 89, 141914 (2006). doi:10.1063/1.2358113.
7. J.W. Jang, P.G. Kim, K.N. Tu, D.R. Frear, and P. Thompson, *J. Appl. Phys.* 85, 8456 (1999). doi:10.1063/1.370627.
8. K.C. Hung, Y.C. Chan, and C.W. Tang, *J. Mater. Sci. Mater. Electron.* 11, 587 (2000). doi:10.1023/A:1008920527395.
9. M. He, Z. Chen, and G.J. Qi, *Acta Mater.* 52, 2047 (2004). doi:10.1016/j.actamat.2003.12.042.
10. A. Kumar, M. He, and Z. Chen, *Surf. Coat. Tech.* 198, 283 (2005). doi:10.1016/j.surfcoat.2004.10.085.
11. M. He, Z. Chen, G.J. Qi, C.C. Wong, and S. Mhaisalkar, *Thin Solid Films* 462, 363 (2004). doi:10.1016/j.tsf.2004.05.045.
12. D.G. Kim, J.W. Kim, J.G. Lee, H. Mori, D.J. Quesnel, and S.B Jung, *J. Alloy. Compd.* 395, 80 (2005). doi:10.1016/j.jallcom.2004.11.038.
13. M. He, W.H. Lau, G.J. Qi, and Z. Chen, *Thin Solid Films* 462, 376 (2004). doi:10.1016/j.tsf.2004.05.058.
14. Z. Mei and R.H. Dauskardt, *MRS Spring Meeting Symposium M: Materials Reliability in Microelectronics IX* (1999), pp. 1–6.
15. M. He, A. Kumar, P.T. Yeo, G.J. Qi, and Z. Chen, *Thin Solid Films* 462, 387 (2004). doi:10.1016/j.tsf.2004.05.062.
16. Z. Chen, M. He, and G.J. Qi, *J. Electron. Mater.* 33, 1465 (2004). doi:10.1007/s11664-004-0088-8.
17. J.F. Li, S.H. Mannan, M.P. Clode, K. Chen, D.C. Whalley, C. Liu, and D.A. Hutt, *Acta Mater.* 55, 737 (2007). doi:10.1016/j.actamat.2006.09.003.
18. M.O. Alam, Y.C. Chan, and K.N. Tu, *J. Appl. Phys.* 94, 4108 (2003). doi:10.1063/1.1602563.
19. Y.D. Jeon, K.W. Paik, K.S. Bok, W.S. Choi, and C.L. Cho, *Proceedings of Electronic Component and Technology Conference* (2001), pp. 1326–1332.
20. M. He, Z. Chen, and G.J. Qi, *Metall. Mater. Trans. A* 36, 65 (2005). doi:10.1007/s11661-005-0139-7.
21. Z. Chen, M. He, A. Kumar, and G.J. Qi, *J. Electron. Mater.* 36, 17 (2007). doi:10.1007/s11664-006-0008-1.
22. Z. Chen, A. Kumar, and M. Mona, *J. Electron. Mater.* 35, 2126 (2006). doi:10.1007/s11664-006-0322-7.
23. A. Kumar and Z. Chen, *IEEE Trans. Compon. Packag. Tech.* 29, 886 (2006). doi:10.1109/TCAPT.2006.886847.
24. A. Kumar, Z. Chen, S.G. Mhaisalkar, C.C. Wong, P.S. Teo, and V. Kripesh, *Thin Solid Films* 504, 410 (2006). doi:10.1016/j.tsf.2005.09.059.
25. A. Kumar and Z. Chen, *Mater. Sci. Eng. A* 423, 175 (2006). doi:10.1016/j.msea.2005.12.040.
26. S.-W. Chen, S.-W. Lee, and M.-C. Yip, *J. Electron. Mater.* 32, 1284 (2003). doi:10.1007/s11664-003-0024-3.
27. A. Sharif and Y.C. Chan, *J. Electron. Mater.* 35, 1812 (2006). doi:10.1007/s11664-006-0162-5.
28. J.-W. Nah, F. Ren, K.-W. Pain, and K.N. Tu, *J. Mater. Res.* 21, 698 (2006). doi:10.1557/jmr.2006.0086.
29. L. Zhang, Z.G. Wang, and J.K. Shang, *Scr. Mater.* 56, 381 (2007). doi:10.1016/j.scriptamat.2006.10.043.
30. B. Vanhecke, L. De Schepper, W. De Ceuninck, V. D'Haeger, M. D'Olieslaegers, E. Beyne, J. Roggen, and L. Stals, *Microelectron. Reliab.* 33, 1141 (1993). doi:10.1016/0026-2714(93)90344-X.
31. A. Kumar, M. He, Z. Chen, and P.S. Teo, *Thin Solid Films* 462, 413 (2004). doi:10.1016/j.tsf.2004.05.042.